NONLINEAR INTERACTION

LASER BEAM WITH SOLIDS

FINAL REPORT

June 30, 1965

Prepared for
THE OFFICE OF NAVAL RESEARCH
on
Contract No. Nonr-1100(24)
Project Code 015-803
ARPA Order No. 306-62

by
A. K. Kamal
and
M. Subramanian

Quantum Electronics Laboratory
SCHOOL OF ELECTRICAL ENGINEERING
Purdue University
Lafayette, Indiana

Period Covered
April 1, 1963 through June 30, 1965

This research is a part of the Project DEFENDER, under the joint sponsorship of the Advanced Research Projects Agency, the Office of Naval Research and the Department of Defense.

NONLINEAR INTERACTION
OF
LASER BEAM WITH SOLIDS

FINAL REPORT
June 30, 1965

Prepared for

THE OFFICE OF NAVAL RESEARCH

on
Contract No. Nonr-1100(24)
Project Code 015-803
ARPA Order No. 306-62

by

A. K. Kamal

and

M. Subramanian

Quantum Electronics Laboratory

School of Electrical Engineering
Purdue University
Lafayette, Indiana

Period Covered
April 1, 1963 through June 30, 1965

This research is a part of the Project DEFENDER, under the joint sponsorship of the Advanced Research Projects Agency, the Office of Naval Research and the Department of Defense.

TABLE OF CONTENTS

Page

Abstract.. ii

1. Introduction.................................... 1

2. Nonlinear D.C. Polarization at Optical Frequencies.. 4

3. Optical Subharmonic Generation.................. 18

Acknowledgements.................................. 25

References.. 26

Figures...

Distribution List.................................

ABSTRACT

This project deals with two types of nonlinear interaction of intense laser beam with dielectric medium. The first and extensively studied phenomenon is the nonlinear dc polarization that is caused by the second order nonlinear polarization. The quartz crystal is chosen as the dielectric medium. A quantitative relationship between the dc polarization and the intensity of the propagating laser beam is given. A convenient method of detecting dc polarization is presented. With this technique the elements of the second order polarization coefficient can be determined experimentally. By considering a suitable detecting system with a convenient configuration of the quartz crystal, it is shown that the output voltage of the detector is linearly proportional to the intensity of the laser pulse. Thus, the possibility of using this principle to build a transmission type of meter for measuring power in high-power laser pulses is presented. Preliminary experimental results on the correlation between the spikings in the dc polarization and in the fundamental frequency of laser oscillation are presented.

The second type of nonlinear polarization presented in this report is the initiation of a study on the generation of subharmonics at optical frequencies using high intensity laser sources. The physical mechanism that is utilized for this purpose is the nonlinear interaction of electromagnetic

radiation with certain types of crystalline media such as quartz and KDP. This nonlinear interaction results in parametric sub-harmonic generation under favorable conditions. The experimental arrangement used for this investigation is outlined.

1. INTRODUCTION

The purpose of this project was to study the nonlinear polarization effects in crystals when high intensity electromagnetic wave propagates through them. This was made possible by the availability of high power lasers. Two types of nonlinearities are treated in this report. They are:

1. Second order nonlinear d.c. polarization.
2. Generation of subharmonics due to nonlinear polarization.

The earliest result of the efforts in the investigation of nonlinear polarization using laser beams was reported by Franken, et. al.[1]. They observed second harmonic generation by passing ruby laser beam through crystalline quartz medium. The production of second harmonic can be explained by considering the following simple scalar mathematical model relating the polarization p and the electric field intensity E.

$$p = a_1 E + a_2 E^2 + a_3 E^3 + \dots\dots\dots\dots \qquad (1)$$

Here a_1, a_2, a_3, ... are called the first, second, third, ... order polarization coefficients. In writing Eq. (1) the gradients of the E field have been neglected for simplicity. If the electric field is caused by the laser beam, E can be written as $E = E_o \cos \omega t$, ω being the angular frequency of the radiation field. Substituting this value of E in Eq. (1), one has

$$p = a_1 E_o \cos \omega t + \frac{a_2}{2} E_o^2 (1 + \cos 2\omega t)$$
$$+ \frac{a_3}{4} E_o^3 (3 \cos \omega t + \cos 3\omega t) + \ldots.. \quad (2)$$

It can be readily observed that the second term in the right hand side of Eq. (2) generates the second harmonic. In general, the coefficients a_1, a_2, a_3, ... are tensors. However, a discussion of their tensor form is deferred. Franken and Ward[2] have shown in detail that the coefficient a_2 will be nonzero only in those media which posses lack of inversion Symmetry.

From Eq. (2) it can be seen that the second harmonic generation is accompanied by a d.c. component. Thus, the successful observation of the second harmonic output initiated interest in investigating the d.c. polarization. Bass, et. al.[3] have reported observing the d.c. polarization in KDP and KD_2P crystals. The authors[4] have applied this phenomenon in quartz crystal for laser power measurement. Section 2 of this report presents the details of the extensive work that was performed on the d.c. polarization.

The preliminary investigation made to generate subharmonics using high intensity laser sources is presented in Section 3. The subject of subharmonic oscillation has been dealt with by various authors[2,5,6]. Armstrong, et.al.[5], and Franken and Ward[2] have considered the propagation of three signals through a nonlinear medium. Under degenerate conditions, energy is transferred from a signal at frequency 2ω to the signal at frequency ω. Kingston and McWhorter have analyzed the problem using coupled mode theory. Up to the present time, to the best of the authors' knowledge, no experimental evidence of the existence of optical subharmonics has been demonstrated, and our efforts are aimed toward this goal.

2. NONLINEAR D.C. POLARIZATION AT OPTICAL FREQUENCIES

2.1 Introduction

The generalized expression for polarization, in the absence of any external biasing electric or magnetic field, may be written as a power series in terms of the components of the electric field intensity and its gradient.

$$p_i = \varepsilon_o \left[X_{ij} E_j + X'_{ijk} \nabla_j E_k + X''_{ijk} E_j E_k + X'''_{ijk\ell} E_j \nabla_k E_\ell + X''''_{ijk\ell} E_j E_k E_\ell + \ldots\ldots\ldots \right] \qquad (3)$$

where p_i is the i^{th} spatial component of polarization p, X's represent the various orders of polarization coefficient tensors, ∇'s denote the gradient operation, E's are the spatial components of the electric field intensity and ε_o the free space permittivity. Franken and Ward[2] have discussed the physical significance of the various terms in Eq. (3). It is enough to mention here that the only term in the right hand side that can cause d.c. polarization in the medium is the second order term $X''_{ijk} E_j E_k$. The magnitude of d.c. polarization due to terms of higher order than those in Eq. (3) can be neglected as compared with that of the second order term since the contribution to polarization decreases as the ratio of the electric field intensity E of the electromagnetic wave to the atomic electric field intensity E_{atomic} (E/E_{atomic}) for each additional E factor added[2].

Retaining only the second order term, Eq. (3) can be written as

$$p_i = X_{ijk} E_j E_k \tag{4}$$

where X_{ijk} is a third rank tensor. It will be shown in Section 2.9 that the second order polarization tensor is related to the linear electro-optic tensor. The experimental results of Bass, et. al.[3] on KDP and KD_2P crystals and one of the results presented in this report confirms the above theory.

This section deals with the observation of the d.c. polarization in quartz crystal and by measurement of this d.c. polarization, calculating one of the second order nonlinear polarization coefficients. The theory of the propagation of the laser beam along the optic axis of the quartz dielectric medium has been treated elsewhere[4] and a brief review is given in Section 2.2. The d.c. polarization developed by the laser beam is detected due to its interaction with an external detecting system. This is explained in Section 2.3 by assuming a simplified model. The equivalent circuit representation is then derived for the system. From both the circuitry and field theory aspects, it is shown that no energy conversion is possible from optical frequency to d.c. by making use of this phenomenon. In Sections 2.4 and 2.5, the theoretical and constructional details of the quartz detector are presented. The experimental arrangement and results on quartz crystal are given in Section 2.6. The results of Sections 2.7, 2.8 and 2.9 include the observation of d.c.

polarization, its angular dependence with respect to crystal axes orientation and the estimation of the second order nonlinear polarization coefficient. Section 2.10 gives the experimental results of the spiking phenomenon in the d.c. polarization. The results are summarized in Section 2.11.

2.2 Propagation in an Infinite Medium

The propagation of an electromagnetic wave through a nonlinear medium has already been discussed in detail by various authors[5,7] from both the quantum mechanical and phenomenological approaches. When considering the interaction between various waves propagating in a medium, one has to take into account such effects as the dispersion in the medium, the phase matching of the various components and so forth. However, in the case of d.c., the phase velocity is infinite and there is no propagation of wave at zero frequency. An analysis for the d.c. case has been presented by the authors elsewhere[4] and only a brief summary is presented here.

The nonlinear dielectric considered is crystalline quartz. The medium is assumed to be infinite in extent and non-dissipative. The second order polarization tensor and the piezoelectric tensor, both of rank 3, are determined by the same symmetry conditions and hence have the same form. Thus, the following contracted form of the piezoelectric notation[8] can be used to write X_{ijk} in Eq. (4).

$$X_{ijk} \rightarrow X_{ij} \quad (i = 1, 2, 3; \; j = 1, 2, \ldots\ldots, 6) \qquad (5)$$

For quartz crystal belonging to class 32, X_{ij} can be expressed in the form similar to its piezoelectric tensor[9] which is shown below.

$$X_{ij} = \frac{1}{\varepsilon_o} \begin{pmatrix} \alpha & -\alpha & 0 & \beta & 0 & 0 \\ 0 & 0 & 0 & 0 & -\beta & -2\alpha \\ 0 & 0 & 0 & 0 & 0 & 0 \end{pmatrix} \qquad (6)$$

From Eqs. (4), (5), and (6)

$$p_x = \alpha(E_x^2 - E_y^2) + \beta E_y E_z$$

$$p_y = -\beta E_y E_z - 2\alpha E_x E_y \qquad (7)$$

$$p_z = 0$$

The special case of propagation along the optic axis will now be considered. The orientation of the crystal axes and the direction of polarization of the beam are shown in Figure 1. The laser beam is assumed to be linearly polarized in a direction making an angle θ with the x-axis of the crystal. In Figure 1, x'x' and y'y' are arbitrary choices of coordinate axes, and xx and yy are the cyrstal axes. Then, it can be shown[4] that the d.c. polarization along the two crystal axes are given by

$$p_x = \frac{\alpha E_o^2}{2} \cos 2\theta \qquad (8)$$

$$p_y = \frac{\alpha E_o^2}{2} \sin 2\theta \qquad (9)$$

where $E = E_o \cos \omega t$ is the electric field intensity of the incident radiation. Figure 1 along with Eqs (8) and (9) describe the angular dependence of d.c. polarization. It can be observed that as the direction of polarization of the incident radiation is rotated through an angle θ, the d.c. polarization is rotated through an angle 2θ in the opposite direction.

2.3 Detecting Technique and Circuit Considerations

This section is devoted to the technique by which the d.c. polarization is detected and an equivalent circuit model is developed for the detecting system. In order to develop the concept, a simple model is chosen and an analysis of it is made.

The nonlinear polarization can be detected with the use of an external circuit arrangement of the type described below. The medium in which the nonlinear polarization is established is made part of a capacitor that is formed by two electrodes that are placed on opposite sides of the dielectric. The capacitor thus formed is then connected to an external detector. The arrangement shown in Figure 2 represents the simple case of a parallel plate capacitor formed with the nonlinear dielectric medium.

The voltage V_Q across the capacitor, neglecting the fringe-effects is given by

$$V_Q = \frac{2P_o d}{\varepsilon} \tag{10}$$

where P_o is the uniform polarization induced by the laser beam in the entire dielectric medium along y-direction, 2d the thickness of the dielectric and is also the distance between capacitor plates, and ε the permittivity of the dielectric at low frequencies.

The capacitor shown in Figure 2 is now connected to an external detector with an input capacitance C and an input resistance R. The nodal equation at node A is

$$\frac{dQ}{dt} + \frac{V_o}{R} + C\,\frac{dV_o}{dt} = 0 \qquad (11)$$

where V_o is the instantaneous voltage across the capacitor plates and +Q and -Q are the charges on them. The charge Q on each plate is due to the external polarization source plus the depolarizing effect in the material. Assuming unit area for the capacitor plate, the total charge on the capacitor is

$$Q = \varepsilon E + P_o \qquad (12)$$

where E is the electric field intensity in the capacitor. Substituting Eq. (12) in Eq. (11), one has

$$\frac{dV_o}{dt}\left(\frac{\varepsilon}{2d} + C\right) + \frac{V_o}{R} + \frac{dP_o}{dt} = 0 \qquad (13)$$

where E has been replaced by $V_o/2d$. For the nonfringing case that is under consideration, $\varepsilon/2d$ is the capacitance of the capacitor formed with the nonlinear dielectric. If this capacitance is designated by C_Q then Eq. (13) can be rewritten as

$$\frac{dV_o}{dt} + \frac{V_o}{(C_Q+C)\,R} + \frac{1}{(C_Q+C)}\,\frac{dP_o}{dt} = 0 \qquad (14)$$

Now, P_o can be related to V_Q from Eq. (10) by

$$P_o = V_Q\,C_Q' \qquad (15)$$

where C_Q' is an equivalent capacitance and is given by

$$C_Q' = \frac{\varepsilon}{2d} = C_Q \tag{16}$$

Although C_Q' and C_Q are equal in the present case, it need not be the case always. If, for example, there is an air gap between the plate and the dielectric, C_Q' and C_Q will be different. One has to distinguish this difference in an actual system. From Eqs. (14) and (15), the equivalent circuit for the system shown in Figure 3 can be synthesized and is given in Figure 4. It can be seen that the available polarization source voltage V_e is less than V_Q, since $C_Q' < C_Q$ and is given by

$$V_e = V_Q \frac{C_Q'}{C_Q} \tag{17}$$

The output response to a continuous laser beam that is turned on at time t = 0, is given in Figure 5. It is seen that the output voltage reduces to zero exponentially. Thus, no continuous d.c. power is delivered to the output except during the transient condition; that is, no optical power rectification is possible. This could also be explained from the field theory point of view. The network done by the field on the system is given by $[\vec{E} \cdot \frac{\partial \vec{P}}{\partial t}]$. For d.c. polarization $\frac{\partial \vec{P}}{\partial t} = 0$ and hence there is no net energy transfer in the steady state condition.

2.4 Theory on the Quartz Detector

In this section a suitable configuration of electrodes is determined for the type of the detector described in the previous section. Consider a circular cylindrical quartz rod with the optic axis oriented along the length of the rod. Let the laser beam propagate along the axial direction. Figure 6 shows the cross-section of the cylindrical quartz rod of radius b with its optic axis perpendicular to the plane of the paper. The incident beam is assumed to be linearly polarized and cylindrical in cross-section. The radius of the beam is a.

Let the laser beam cause a uniform d.c. polarization given by Eqs. (8) and (9) in the transverse direction making an angle ϕ with the axis of the crystal. Since quartz is a uniaxial crystal, the x-y plane is isotropic. This can be considered as a two-dimensional electrostatic problem which has already been solved[4]. The potential outside the crystal is given by

$$V = \frac{\alpha\eta}{\pi\,\varepsilon_o\,(\varepsilon_r + 1)}\; P_L\,\frac{1}{r}\cos(\theta-\phi) \tag{18}$$

where α is the nonlinear polarization coefficient described in Eq. (6), η is the intrinsic impedance of the quartz medium, ε_o is the free-space permittivity, ε_r the relative dielectric constant of quartz at low frequencies and P_L is the intensity of the laser beam. The equipotential lines described by Eq. (18) with $\phi = 0$, are shown in Figure 7. It can be observed that the equation $r = k \cos\theta$. where k is an arbitrary constant, describes equipotential surfaces which are pairs of circles. For the construction of the detector, one such pair corresponding to $r = k_1 \cos\theta$ is chosen. Then the voltage across the plates is given

$$V_Q = KP_L \tag{19}$$

where

$$K = \frac{2\alpha\eta}{k_1 \pi \varepsilon_o(\varepsilon_r + 1)} \tag{20}$$

2.5 Construction of the Quartz Detector Mount

The perspective view of the quartz detector mount which is an assembly of the crystal holder, rotating mechanism and the built-in pre-amplifier, is shown in Figure 8. A metallic cylinder encloses a plastic cyrstal holder with electrodes and the preamplifier. The preamplifier is mounted on the rear of the cylinder. The metal cylinder is supported at the ends by two flanges mounted on a common base such that it can be rotated about its axis. The holes on the front and rear end of the cylinder permit the laser beam to travel through the crystal and out without any obstruction.

A cut-away view of the crystal holder and electrode assembly is shown in Figure 9. This part of the assembly is made with insulator material to minimize any disturbance of the potential field configuration set up by the d.c. polarization. The two flanges with circular holes at the center keep the cylindrical crystal in position and do not interfere with the path of the laser beam.

The primary requirements of the preamplifier are that it should have a high input impedance and low noise figure. A balanced cathode follower using the subminiature tube CK 6112 is built inside the mount. The filament is operated from a d.c. source and the tube is operated under heavy space charge conditions.

2.6 Experimental Arrangements

The general set up of the experiment is shown in Figure 10. The experiment is conducted with a pulsed ruby laser than can deliver approximately one joule of energy output with a pulse width of approximately 400 microseconds. The output from laser is passed through the quartz detector. The quartz detector mount has facility for vertical, transverse and rotational alighments. The beam emerging from the detector strikes a white background. The scattered light is picked up by a photomultiplier and is fed to one of the inputs of the dual beam oscilloscope (Tektronix Model 555). The output of the quartz detector is fed to the second input of the oscilloscope. Both traces of the oscilloscope are synchronized with the trigger voltage that fires the laser. The oscilloscope is set for single sweep operation.

2.7 Observation of D.C. Polarization

With the set up shown in Figure 10, the quartz output was measured. The output is of the order of 40 microvolts. This is for the angular position of the mount for which the output is positive maximum. Figure 11a is the oscilloscope picture showing this output. The upper trace is the photomultiplier output representing the laser output. The photomultiplier tube circuit has a long time constant and hence the spikes in the ruby output are not seen. Only the envelope of the laser output is present. The lower trace represents the quartz detector output at the position of maximum positive output. Here also one does not see the spikes though they are present, due to limited bandwidth of the prea 'fier. Figure 11b represents the situation when the quartz crystal is replaced by a glass rod. The angular position of the quartz mount is maintained the same as in the earlier case. The output of the quartz was due to its crystalline character. However, glass is amorphous and should yield no output. Thus, a comparison of the two output proves that the output voltage is due to the crystalline nature of the medium. In Figure 11b one observes a very small output from the glass rod which is found to be independent of the angular position. This small output might be due to the residual strain in the glass rod.

2.8 Angular Dependence of D.C. Polarization

It was proved in Section 2 that rotating the quartz detector about its axis while keeping the electric field orientation of the laser beam fixed in space, the d.c. polarization should rotate at double the angular rate. Thus, if the quartz detector is rotated through 90° in either clockwise or anti-clockwise direction the d.c. polarization vector should rotate through an angle of 180°. This means that one should expect a reversal in the d.c. output voltage of the quartz detector as it is rotated through 90°. This is proved by the pictures shown in Figure 12. Figure 12a represents an angular position for which the output is a negative maximum. Figure 12b represents the angular position 90° away from that corresponding to Figure 12a. It is seen that for the same laser power, depicted by the upper traces, the magnitude of the quartz output remains the same while the direction alone reverses.

2.9 Determination of Second Order Nonlinear Coefficient

It is possible to estimate the value of the second order nonlinear coefficient α in the matrix of Eq. (6) by measuring the d.c. output voltage of the quartz detector. The procedure is to first determine the peak power in the laser pulse by measuring the total energy using calorimetric technique and knowing the pulse shape given by the photomultiplier output. Knowing this value of P_L in Eq. (19) and the circuit parameters in Figure 4, α can be calculated directly. The value obtained in this experiment is 1.18×10^{-8} e.s.u.* In obtaining this value, correction has been made for the presence of optical activity in quartz. It can be shown[10] that the maximum corrected polarization due to optical activity will be 0.38 times that of uncorrected value.

It was mentioned in Section 2.1 that the second order nonlinear polarization coefficient was related to the electro-optic coefficients. This has been worked out in detail by Bass[12]. Following this approach it can be shown[10] that α is given by

$$\alpha = \frac{n_o^4}{32\pi} \; r_{11} = 0.28 \times 10^{-8} \text{ e.s.u.}$$

where n_o is the ordinary index of refraction and r_{11} the electro-optic coefficient. Comparing this with the experimental value, it is seen that the measured value is approximately four times that of the theoretical value. This is attributed to the errors

---

* This value is different from that quoted in Reference 11, because there was an error of a factor of 6 in the initial measurement of power. Also the reduction in polarization due to optical activity was not accounted for originally.

in measurements of the exact value of d.c. polarization and the peak power in the laser.

2.10 Spikings in the D.C. Polarization

The experimental results of the previous sections were obtained using a low power laser. Consequently, the output of the quartz detector was low. The gain-bandwidth criteria of the detecting system precluded the possibility of the observation of the spiking phenomena which occurs at intervals of the order of a microsecond in the d.c. output. Because of the interest in the feasibility of using this method to measure power in the laser beam, a high power laser that is capable of delivering 100 joules output for 500 microseconds was developed. (It should be borne in mind that a Q-switched laser will not serve the present purpose. This is due to the fact that the Q-switched laser delivers much higher intensity for a very short duration and thus the gain-bandwidth requirements of the detecting system has the same restrictions.) Now that the d.c. output was large, a new amplifier using RCA 8056 nuvistors was built which had higher bandwidth and gain. The amplifier circuit diagram is shown in Figure 13. The 8056 nuvistors were chosen because of their small size and electrical properties. They are low noise, high frequency, tubes capable of operating with 10^7 ohm grid resistors. To achieve gain in the input stage and still avoid the Miller effect capacitance, a cascode configuration is used.

The observed spikings in the d.c. polarization are shown in Figure 14. Both in Figures 14a and 14b, the upper trace represents the d.c. output and the lower trace the laser output. It can be observed that the spikings in the d.c. polarizations are rounded off due to bandwidth limitation in the detecting system. Also, according to our preliminary results, we do not see any systematic correlation in amplitudes between the fundamental and d.c. spikings.

2.11 Summary

The d.c. polarization that is developed in a nonlinear dielectric medium of quartz, when a high intensity laser beam propagates through it is investigated. A linear relationship between laser intensity and d.c. polarization is derived for the case of z-axis propagation. A convenient method to detect the d.c. polarization is suggested. The interaction between the propagating wave and the detecting circuitry is analyzed and an equivalent circuit model developed. It is proved that the phenomenon of d.c. polarization cannot transfer any d.c. power to circuitry from the laser beam. Details of the experimental arrangement and the construction of the quartz detector mount are given. The second-order nonlinear polarization coefficient α of quartz is estimated to be 1.18×10^{-8} e.s.u. which is approximately four times the theoretical value predicted. The spikings that are present in the laser can also be observed in the d.c. polarization. However, the preliminary results do not indicate any amplitude correlation between them.

3. OPTICAL SUBHARMONIC GENERATION

3.1 Introduction

At the present time there is a serious gap in signal sources in the frequency range, say 300 to 5,000 kmc. In addition to the academic interest in filling the gap in the electromagnetic spectrum, the availability of signal sources would make possible some interesting new spectroscopic studies of materials. Now that there is available for us very high intensity sources at infra-red frequencies, it strongly suggests the possibility of achieving this goal by generating subharmonics.

The above long-range objective is the motivation for the present study, the purpose of which is to investigate the feasibility of subharmonic generation at optical and infrared frequencies by interaction of a high intensity laser beam with a nonlinear dielectric medium. The principle that is under study is the parametric subharmonic generation.

Interaction of laser beams with nonlinear dielectric media has successfully been employed for the generation of harmonics. We propose here that a similar interaction phenomenon will, under favorable conditions, generate subharmonics of different orders. Specifically, using a crystal that lacks inversion symmetry, a subharmonic which is half the frequency of the laser can be generated. The basic principle of the phenomenon can best be explained by making use of the treatment of parametric oscillations in circuits using varactor diodes (or saturable core inductors). The treatment presented here is of a general nature, instead of a parametric degenerate amplifier, and is intended to illustrate the physical nature of the phenomenon. In what follows, the analogy between an atomic model and circuit theory model for the existence of parametric subharmonic oscillation is presented.

3.2 Theoretical Discussion

3.2.1 Circuit Theory Model[13]

Consider the circuit shown in Figure 15. A varactor (parametric diode) whose capacitance is varied at an angular frequency of 2ω is connected across a parallel resonant circuit. The capacitance of the varactor is given by

$$C(t) = C_o \left(1 + \frac{\Delta C}{C_o} \cos 2\omega t\right) \qquad (21)$$

The resonant frequency of the circuit with $\Delta C = 0$ is given by

$$\omega = \frac{1}{(LC_o)^{1/2}} \qquad (22)$$

If Q_e is the charge on the capacitance, we can write the differential equation which describes the circuit as

$$\frac{d^2Q_e}{dt^2} + \frac{G_e}{C_o}\frac{dQ_e}{dt} + \omega^2 \left(1 - \frac{\Delta C}{C_o} \cos 2\omega t + \ldots\right) Q_e = 0 \qquad (23)$$

Letting $Q_e = e^{-G_e t/2C_o} U(t)$ and neglecting the higher order term inside the parenthesis in Eq. (23), we obtain the canonical Mathieu equation which is of the following form:

$$\frac{d^2U}{dt^2} + (a - 2q \cos 2\omega t)\, U=0 \tag{24}$$

where

$$a = 1 - \frac{G_e^{\ 2}}{4\omega^2 C_o^{\ 2}} \tag{25}$$

$$q = \frac{\Delta C}{4C_o} \tag{26}$$

Equation (24) has two kinds of solutions: stable and unstable. These are described in detail by Chang[13]. For the present discussion, it is enough to mention that under unstable conditions, the circuit sees a negative conductance given by

$$G_n = \frac{\omega\Delta C}{2} \sin 2\phi \tag{27}$$

where ϕ is the phase angle of the subharmonic oscillation. Subharmonic oscillation occurs when $G_n = G_e$.

3.2.2 Interaction of Electromagnetic Radiation with Nonlinear Dielectric Medium

The phenomenon of the interaction of radiation with the nonlinear dielectric medium will be illustrated by considering a one-dimensional anharmonic oscillator that is subjected to the forcing field caused by the radiation. In the absence of radiation, the Hamiltonian of the system is of the form[5]

$$H = \frac{p^2}{2m} + m\omega_o^{\ 2}x^2 - \frac{1}{3}\lambda\, x^3 - \frac{1}{4}\eta x^4 \tag{28}$$

where m is the mass, p the momentum of the particle, λ and η

constants of the system, and x is the displacement of the particle from its equilibrium position. In the electric dipole approximation, the interation of the system with radiation is

$$H_{int} = exE_o \cos(2\omega t + \phi) \tag{29}$$

where e is the electronic charge and $E_o \cos(2\omega t + \phi)$ is the incident monochromatic radiation. From Eqs. (28) and (29) the equation of motion, including a dissipative term, for the system can be written, which will assume a general form as below

$$\frac{d^2x}{dt^2} + \alpha \frac{dx}{dt} + \beta x + \gamma x^2 + \delta x^3 = B \cos 2\omega t \tag{30}$$

Following the procedure of Hayashi[14], assuming a solution of the form

$$x(t) = x_o + k_1 \sin \omega t + k_2 \cos \omega t + k_3 \cos 2\omega t \tag{31}$$

we can obtain from Eq. (30) the following Mathieu equation

$$\frac{d^2U}{dt^2} + \left[\theta_o + 2\sum_{\nu=1}^{4} \theta_\nu \cos(\nu\omega t - \sigma_\nu)\right] U = 0 \tag{32}$$

Hayashi[14] discusses the stability conditions of Eq. (32). Under unstable conditions, the system will oscillate at half the radiation frequency, thus generating subharmonics. We can also recognize this by comparing Eqs. (24) and (32).

3.2.3 Discussion on the Analogy between Circuit and Field Theory Concepts

The above discussion mathematically portrays the similarity between subharmonic generation in circuitry and atomic systems. This can also be explained qualitatively by considering the physical mechanisms. In the circuitry model the varactor capacitance is varied at the pump frequency. This can be visualized as the constant of the dielectric in the capacitor being varied at the pump frequency. In the case of interaction of radiation with the dielectric, the dielectric constant is varied at the radiation frequency due to the second order nonlinear term. That is,

$$\varepsilon = \varepsilon_o + \alpha\, E_o \cos \omega t$$

where ε is the total dielectric constant, ε_o the dielectric constant due to linear term between polarization and electric field intensity, α constant of proportionality and $E_o \cos \omega t$ the radiation field intensity.

Although we have attempted to show the similarity between circuit model and field theory model, we should bear in mind the limitations of extending the concept of circuit theory into the optical region. The availability of high power monochromatic sources at optical and infrared frequencies was a major problem till now. This has been alleviated with the advent of lasers. The second impediment is the proper phase-matching between the fundamental and subharmonic so as to have an efficient transfer of power. The problems involved here are identical to those of the generation of harmonics and have been discussed elsewhere in detail[2,5]. It can, however, be pointed out in our discussion of the analogy, that the phase-matching condition is easily solved in the circuitry by the presence of the idler. In the field-interaction case the extraordinary wave of one frequency is matched to the ordinary wave of the other.

3.3 Experiment

The experimental arrangement is shown in Figure 16. The output of the laser is a collimated beam with a maximum energy of approximately 50 joules. In addition to the laser light the output contains visible and infrared radiation from the flashtubes.

Since the signal to be detected has a wavelength of 1.39μ, the radiation from the flashtubes in this range must be filtered out prior to the anisotropic cyrstal. A four-inch cell filled with glycerin is used for this purpose. A transmission curve for 1.1 cm. of glycerin (in a plexiglass cell) is shown in Figure 17. As can be seen from this curve, the attenuation at 6943 A° is negligible while the attenuation at 1.39μ is very large, approximately 93%.

The attenuation increases exponentially with length. Hence, the four-inch cell attenuates radiation with a wavelength greater than 1.37μ by at least 60 db. The maximum transmission for wavelengths greater than 1.2μ occurs at 1.32μ, and even this is attenuated by more than 30 db. Thus, the primary signal leaving the glycerin cell is the laser beam at 6943 A°.

If the crystal is such that it will support the subharmonic, then the output will consist of the laser beam (very intense) plus the subharmonic of the laser beam. In order to detect the subharmonic signal, the laser beam at 6943 A° and all other radiation outside of a small band at 1.39μ must be suppressed. This is accomplished by a silicon filter.

The band gap energy in pure silicon is 1.1 e.v.; thus silicon has a very high absorption coefficient for radiation with a wavelength of 1.1μ or less. The absorption curve is shown in Figure 18. From measurements made on a 10-mil wafer of silicon, the attenuation of the laser beam in the 3 mm thick disc used should be greater than 180 db.

The use of silicon has disadvantages in that the index of refraction at 1.39μ is 3.97, which means the reflection coefficient is .33. In addition to this, our silicon disc is slightly wedge-shaped and also apparently acts as a scatterer. The net result is an 8 db insertion loss at 1.39μ.

The detection is accomplished by using a PbS photoconductive cell mounted on a three-way positioner so that it may be positioned at the point of maximum signal. The signal waveform is observed on a Tektronix 555 oscilloscope with a Type E head.

As a final prevention against unwanted radiation, a dielectric interference filter will be mounted directly in front of the PbS device.

ACKNOWLEDGEMENTS

The principal investigators express their appreciation to G. L. Fuller, G. L. McAllister and A. Beining for the assistance rendered in performing the experiments and to V. Hendey for partial help in the theoretical analysis. Thanks are due to R. Sciefers, the supervisor of the machine shop for his valuable help in the fabrication of components.

REFERENCES

1. P. A. Franken, A. E. Hill, C. W. Peters and G. Weinreich, "Generation of Optical Harmonics", Phys. Rev. Letters, Vol. 7, No. 4, pp. 118-119, August 15, 1961.

2. P. A. Franken and J. F. Ward, "Optical Harmonics and Nonlinear Phenomena", Revs. Mod. Phys., Vol. 35, No. 1, pp. 23-39, January, 1963.

3. M. Bass, P. A. Franken, J. F. Ward and G. Weinreich, "Optical Rectification," Phys. Rev. Letters, Vol. 9, No. 11, pp. 446-448, December 1, 1962.

4. A. K. Kamal and M. Subramanian, "Laser Power and Energy Measurement Using Nonlinear Polarization in Crystals," Symp. Optical Masers, Polytech. Press, New York, pp. 601-616, (1963).

5. J. A. Armstrong, N. Bloembergen, J. Ducing, and P. S. Pershan, "Interactions Between Light Waves in a Nonlinear Dielectric," Phys. Rev., Vol. 127, No. 6, pp. 1918-1939, September 15, 1962.

6. Kingston, R. H., and McWhorter, A.L., "Electromagnetic Mode Mixing in Nonlinear Media," Proc. IEEE, Vol. 53, No. 1, January, 1965.

7. P. S. Pershan, "Nonlinear Optical Properties of Solids: Energy Considerations," Phys. Rev., Vol. 130, No. 3, pp. 919-929, May 1, 1963.

8. "Standards on Piezoelectric Crystals," Proc. IRE., Vol. 46, p. 764, (1958).

9. J. F. Nye, "Physical Properties of Crystals,"Oxford Press, p. 116, (1957).

10. M. Subramanian and E. V. Hendey," Correction to the Second Order Polarization Coefficient," First Semi-annual Research Summary, July-December 1964, Purdue University School of Electrical Engineering, Lafayette, Indiana.

11. M. Subramanian, "D.C. Polarization in a Nonlinear Dielectric Medium at Optical Frequencies," Doctoral Thesis, Purdue University School of Electrical Engineering, January 1964.

12. M. Bass, "Optical Rectification," Doctoral Thesis, University of Michigan, 1964.

13. Chang, K. K. N., "Parametric and Tunnel Diodes," Ch. 7, Prentice Hall, New Jersey (1964).

14. Hayashi, C., "Nonlinear Oscillations in Physical Systems," Ch. 7, McGraw-Hill, Inc., (1964).

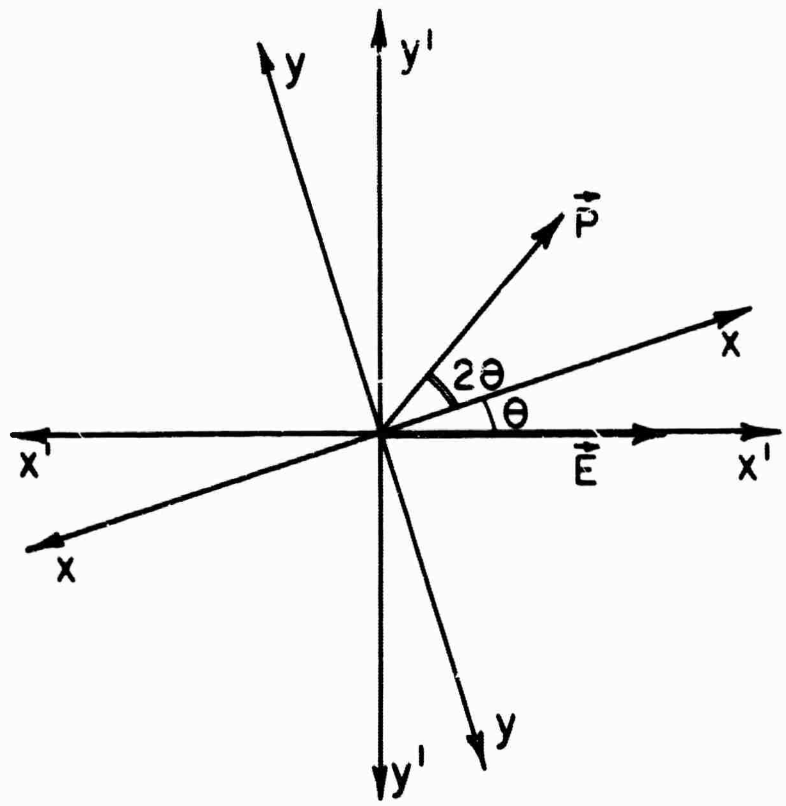

Fig. 1. Axes Orientation for Deriving the Angular Dependence of d. c. Polarization for Propagation Along z-axis

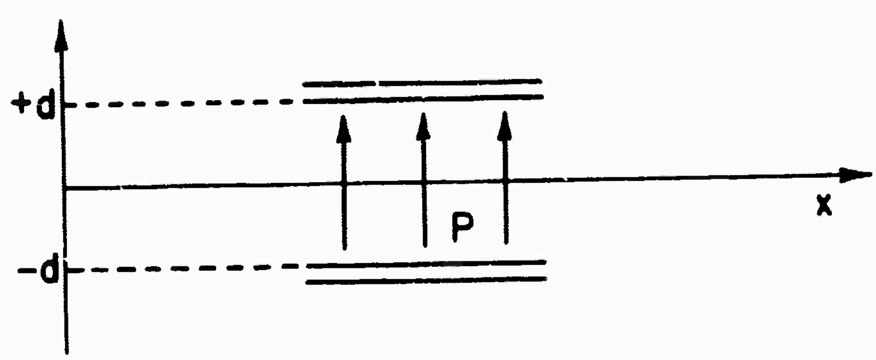

Fig. 2. Simple Parallel Plate Capacitor Formed with the Nonlinear Dielectric. The Polarization P_o is the External Polarization Induced by the Laser Beam.

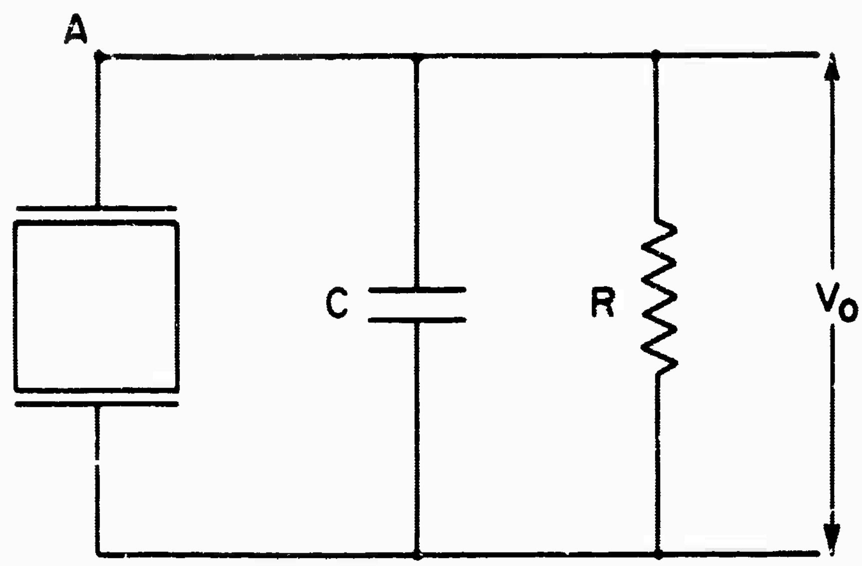

Fig. 3. The Quartz Detector with External Circuitry

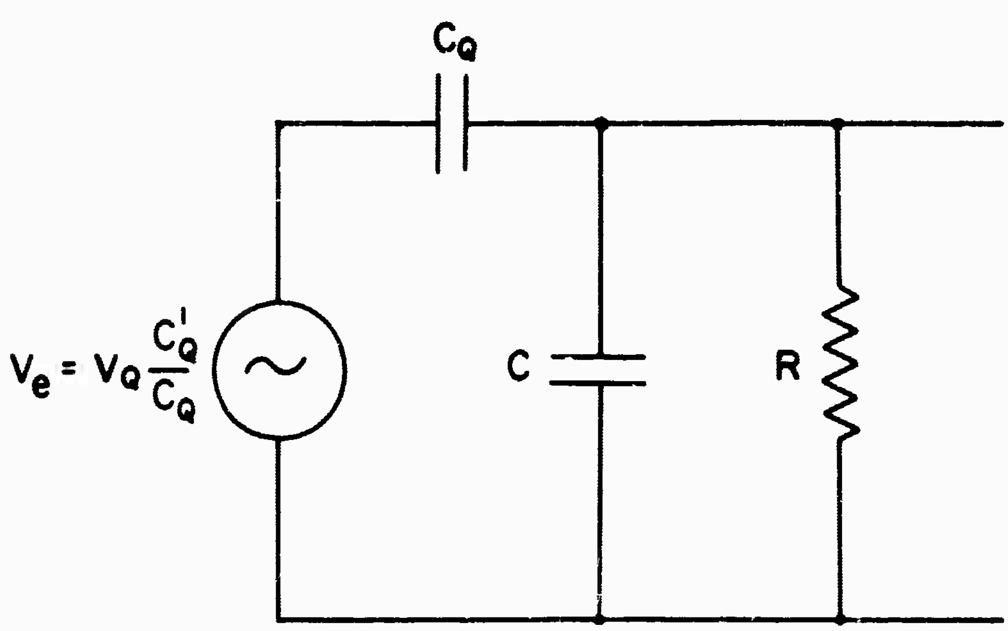

Fig. 4. Equivalent Circuit for the Configuration of Fig. 3

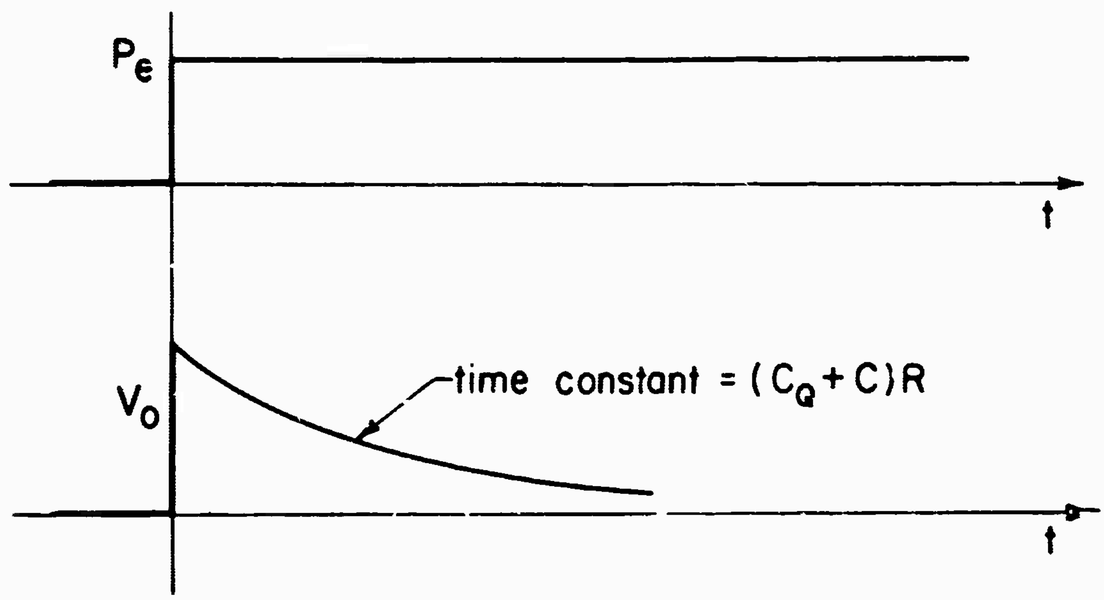

Fig. 5. Output Response to the Step Function of the D.C. Polarization Source.

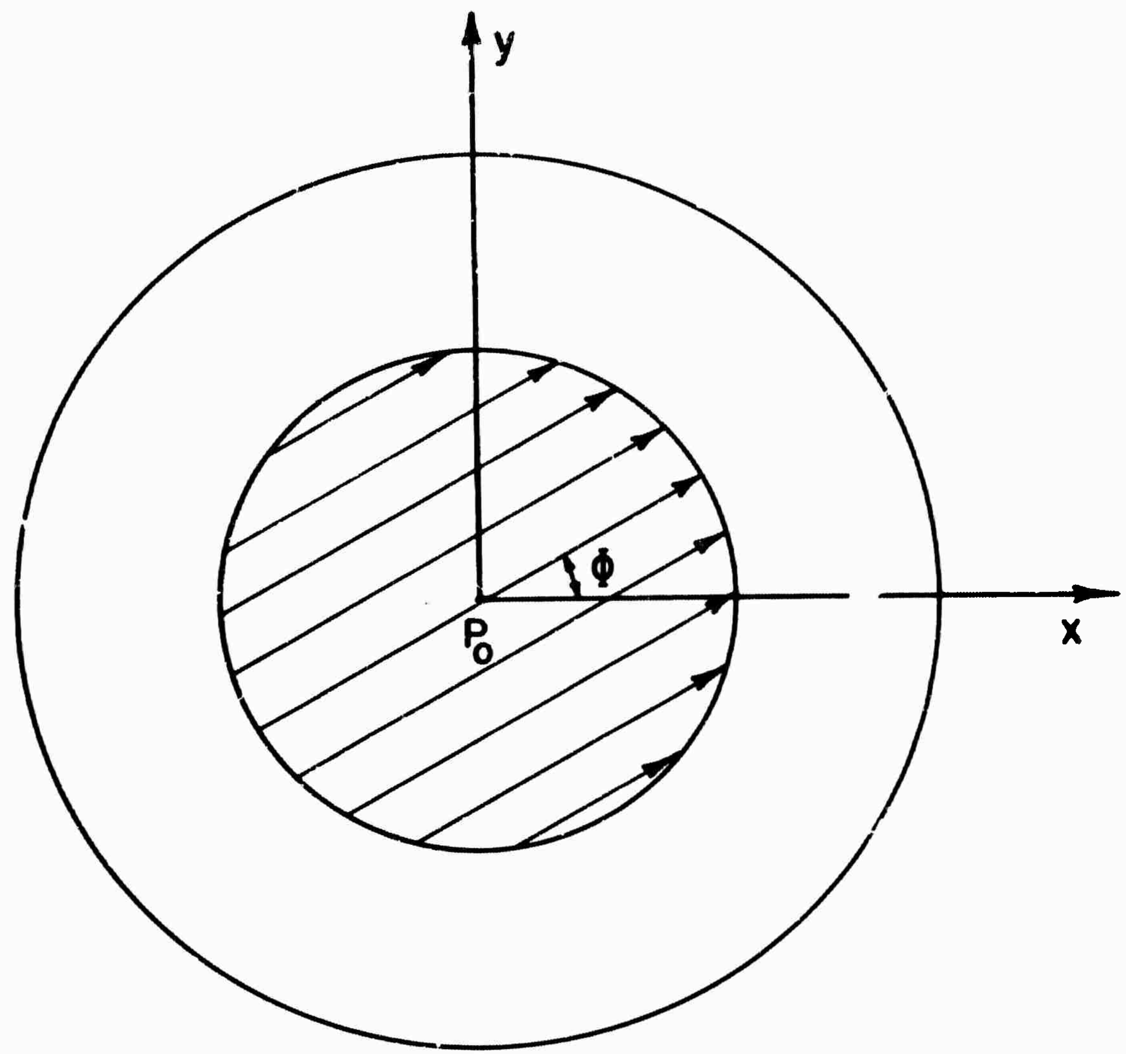

Fig. 6. Cross-Section of the Quartz Rod with Concentric Laser Beam

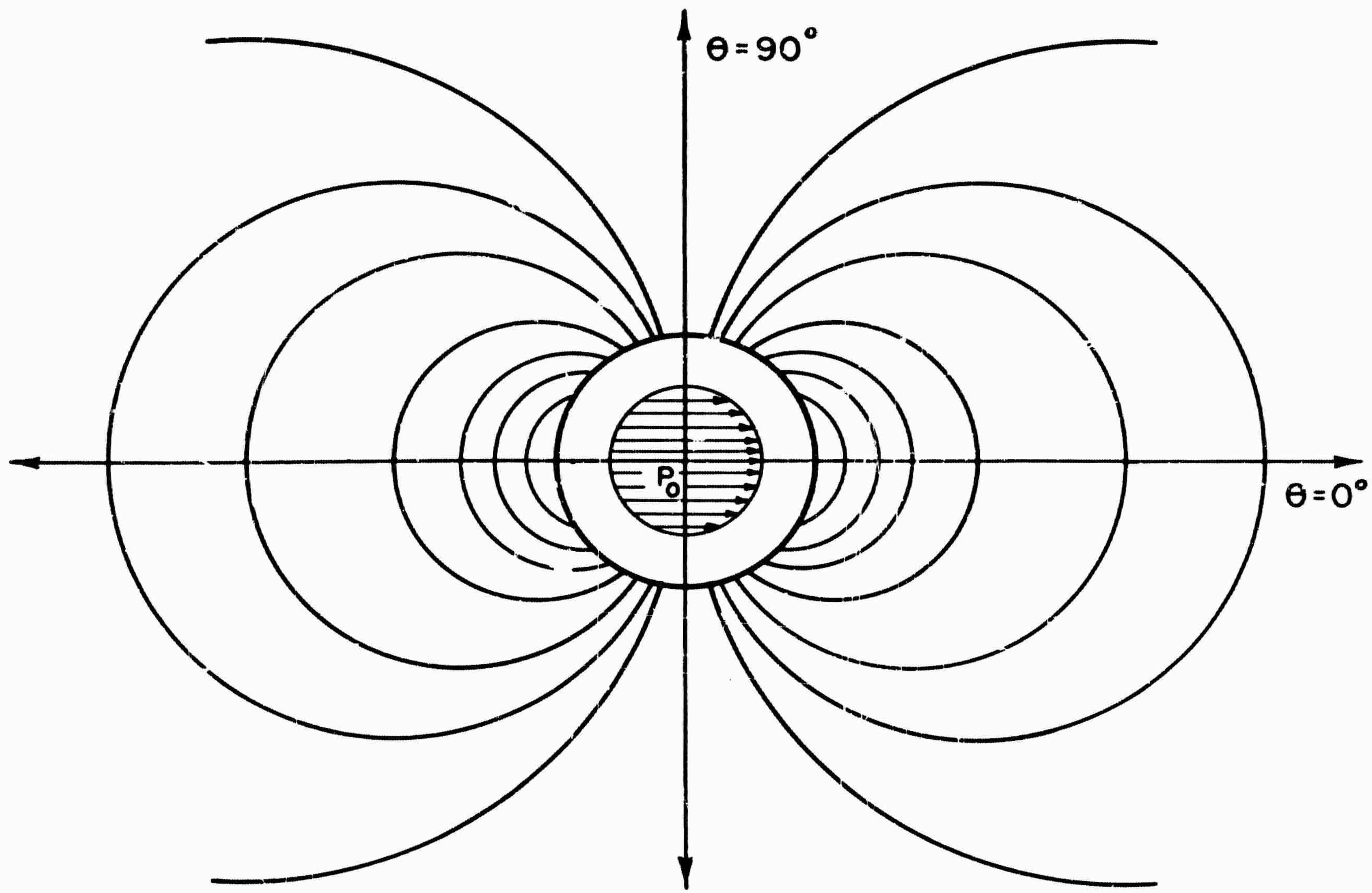

Fig. 7. Equipotential Lines Outside the Quartz Medium

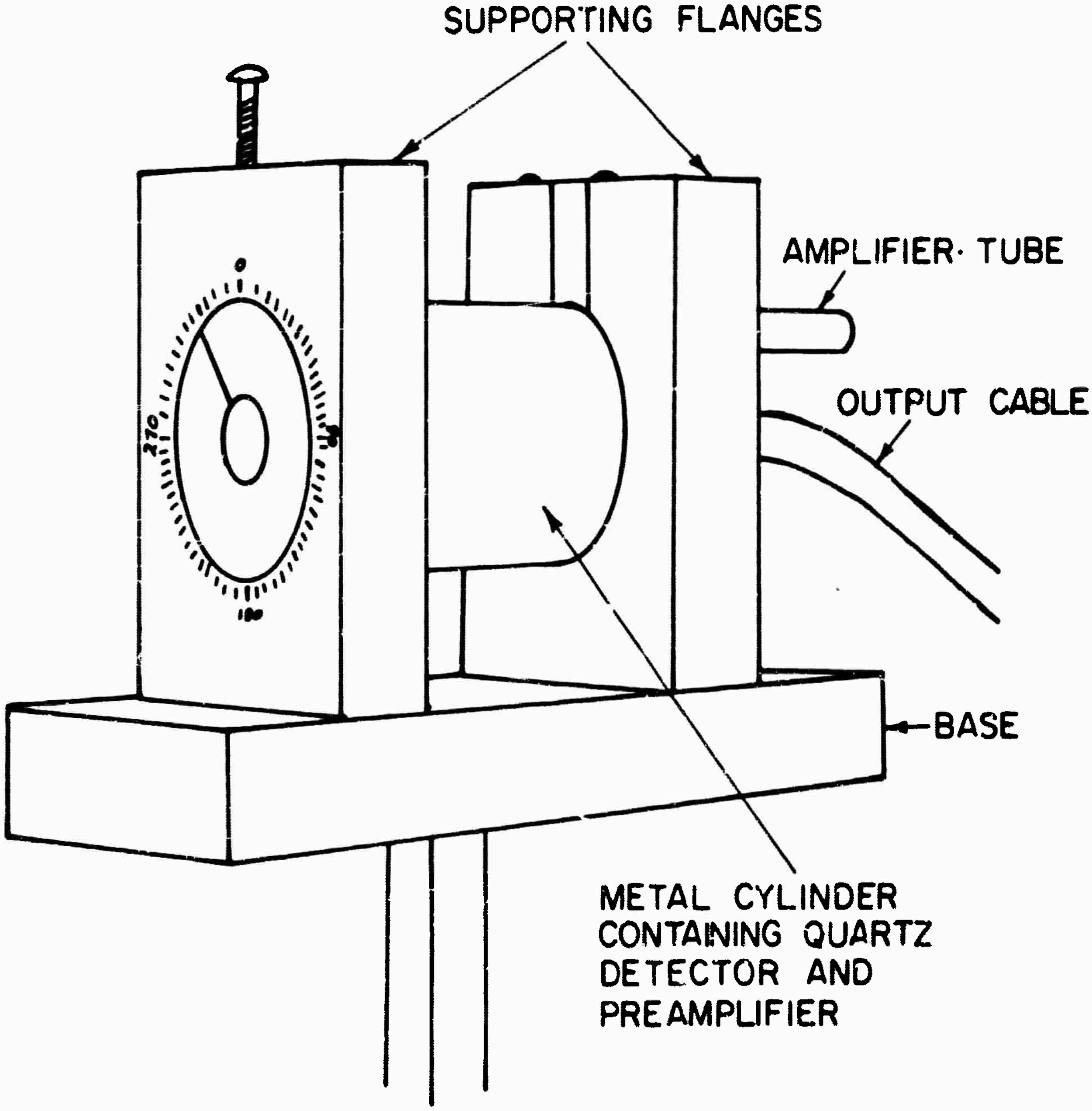

Fig. 8. Perspective View of the Crystal Mount

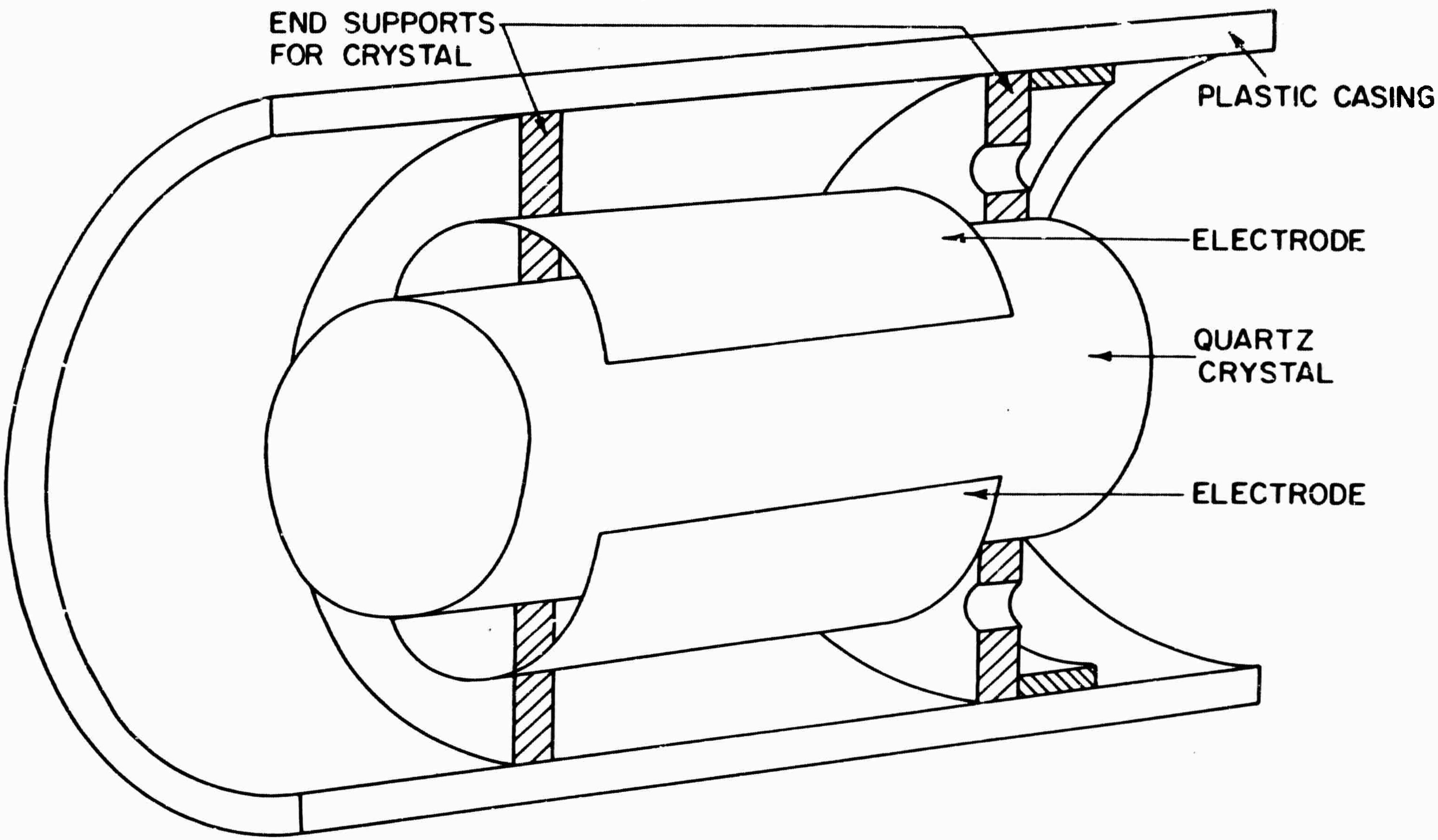

Fig. 9. Cut-Away View of Quartz Detector

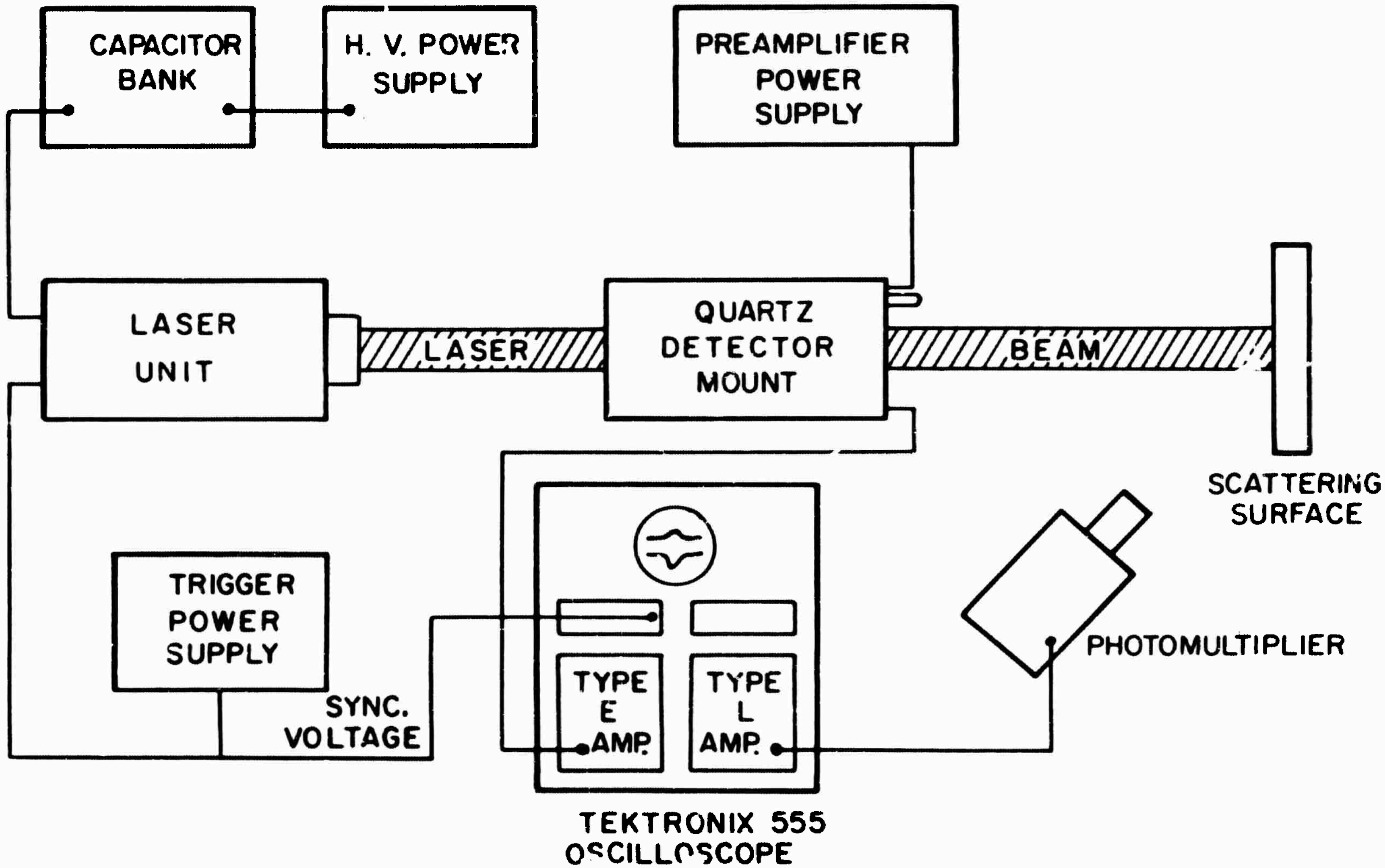

Fig. 10. General Experimental Arrangement

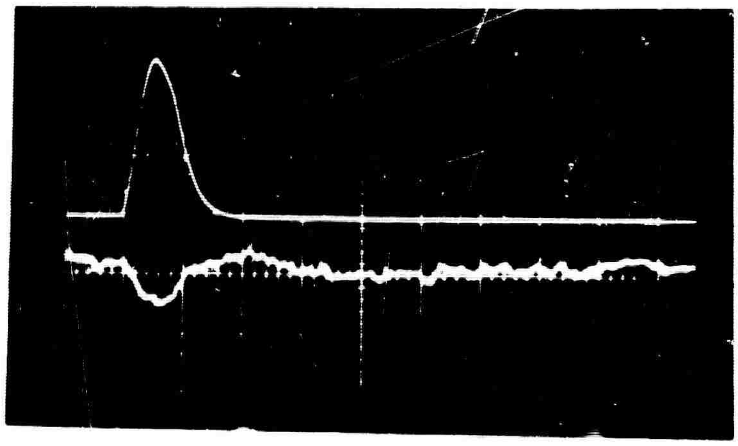

(a)

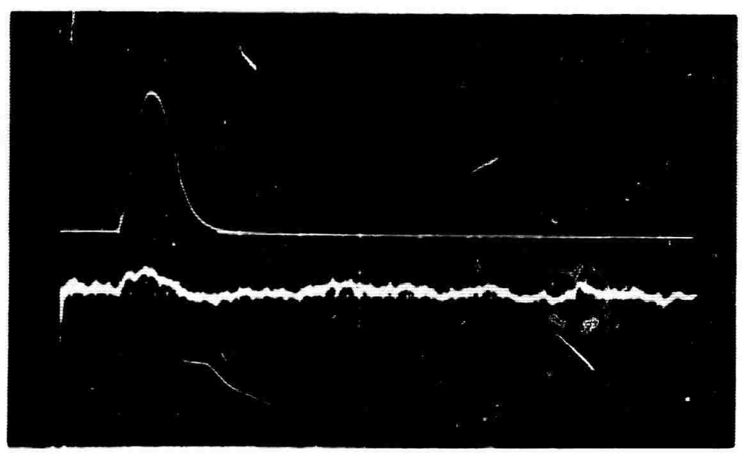

(b)

Fig. 11 Comparison of Output from Quartz Crystal with that from Glass Rod

(a) Photograph of the dual beam oscilloscope in which the lower trace shows the quartz detector output and the upper trace the intensity of the laser beam.
Sweep rate: 500 microseconds/cm.
Sensitivity of upper trace: 50 microvolts/cm.

(b) As in (a) with the quartz replaced by the glass rod.

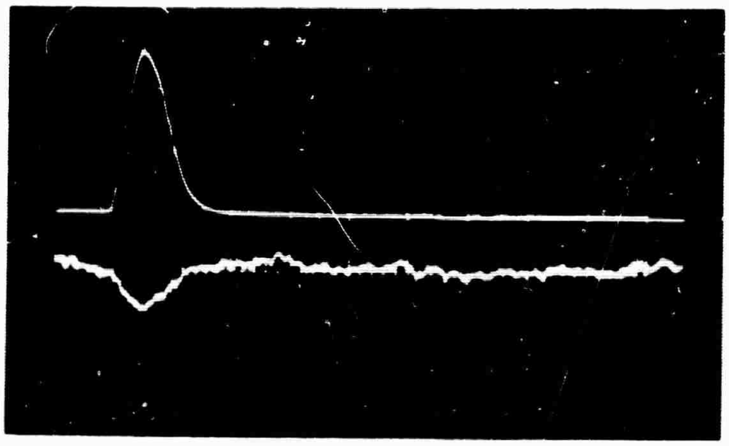

(a)

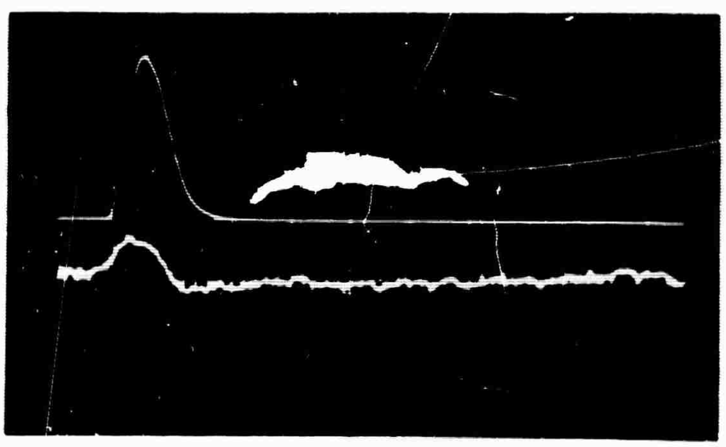

(b)

Fig. 12 Angular Dependence of d.c. Polarization

(a) Photograph of the dual beam oscilloscope in which the lower trace shows the quartz detector output and the upper trace the intensity of the laser beam. Quartz detector is adjusted for maximum negative output.

(b) As in (a); quartz detector rotated by 90° from that of position in (a).

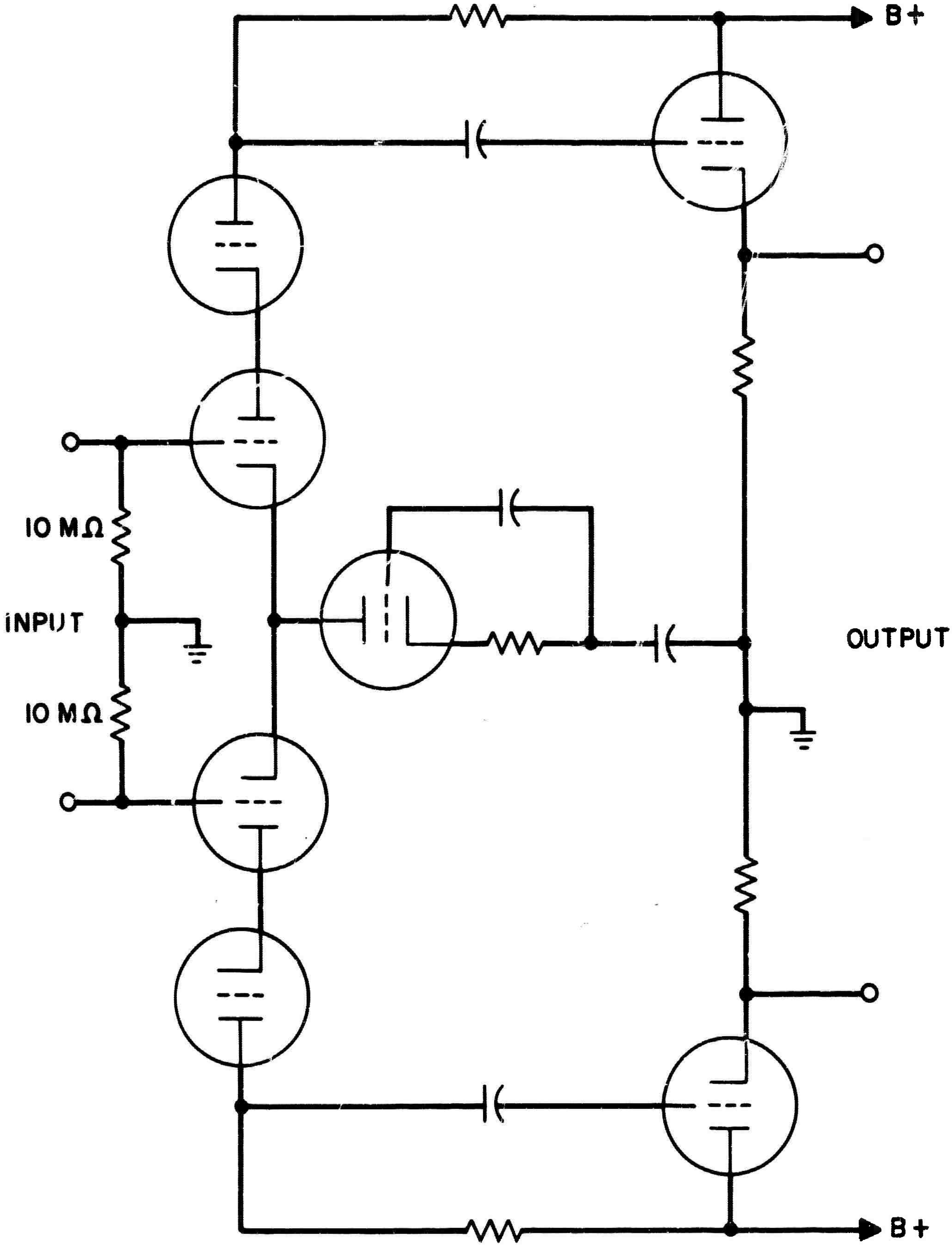

FIG.13 AMPLIFIER USED TO MEASURE SPIKINGS IN THE DC POLARIZATION.

(a)

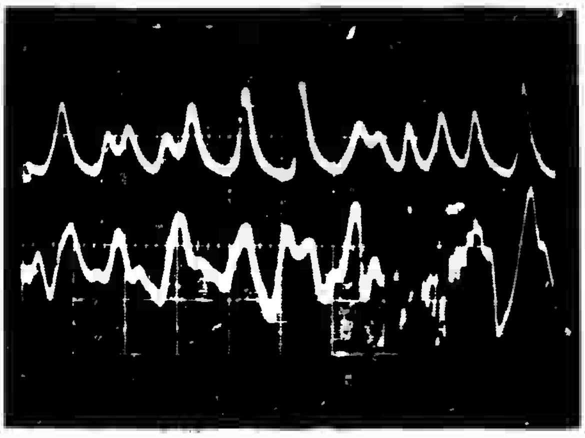

(b)

Fig. 14 Spikings in the d.c. Polarization

(a) Photograph of the dual beam oscilloscope in which the lower trace shows the d.c. polarization and the upper trace the laser output. Time scale: 5 microseconds/cm.

(b) As in (a) with the time scale: 2 microseconds/cm.

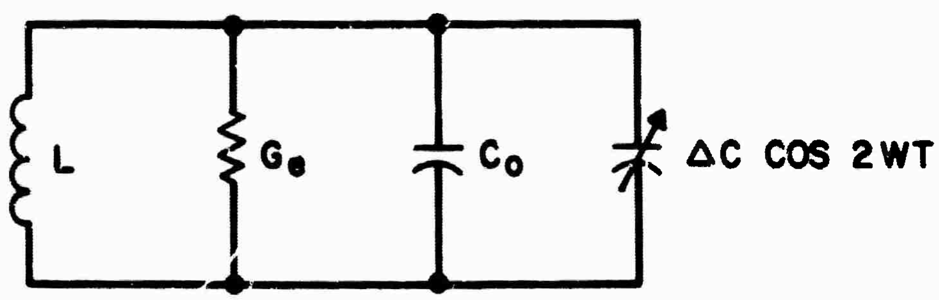

FIG.15 BASIC CIRCUIT FOR SUBHARMONIC GENERATION.

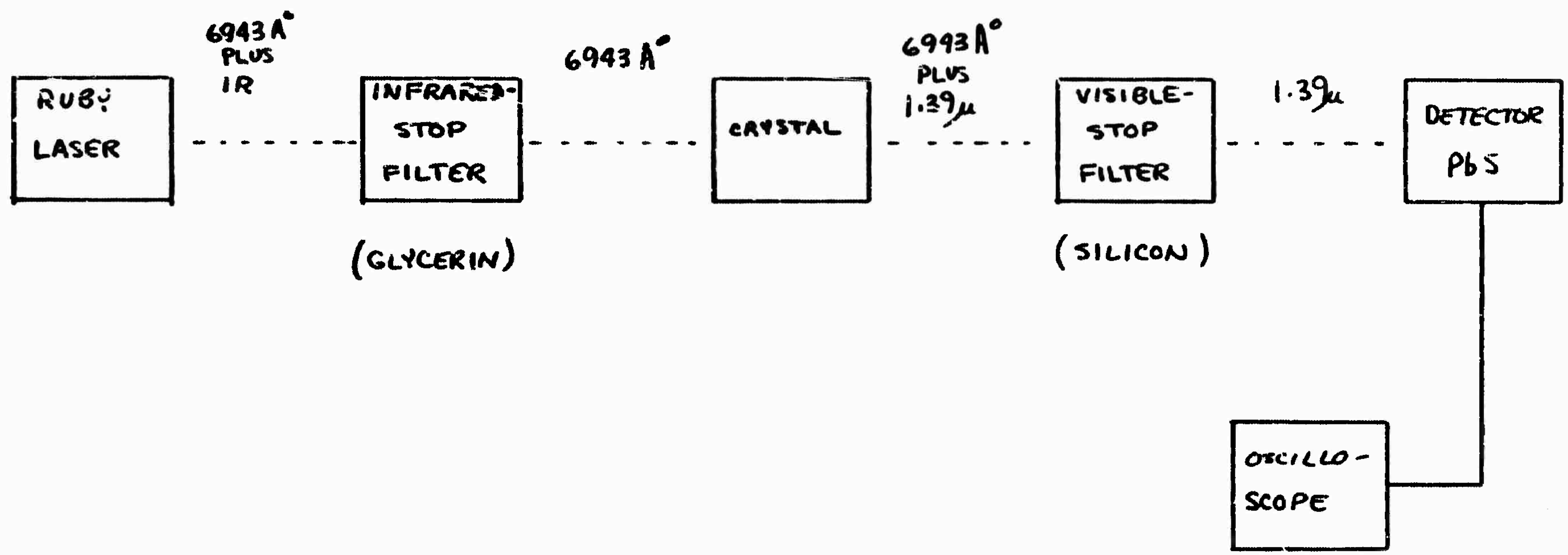

FIGURE 16 EXPERIMENTAL ARRANGEMENT FOR INVESTIGATION OF SUBHARMONICS

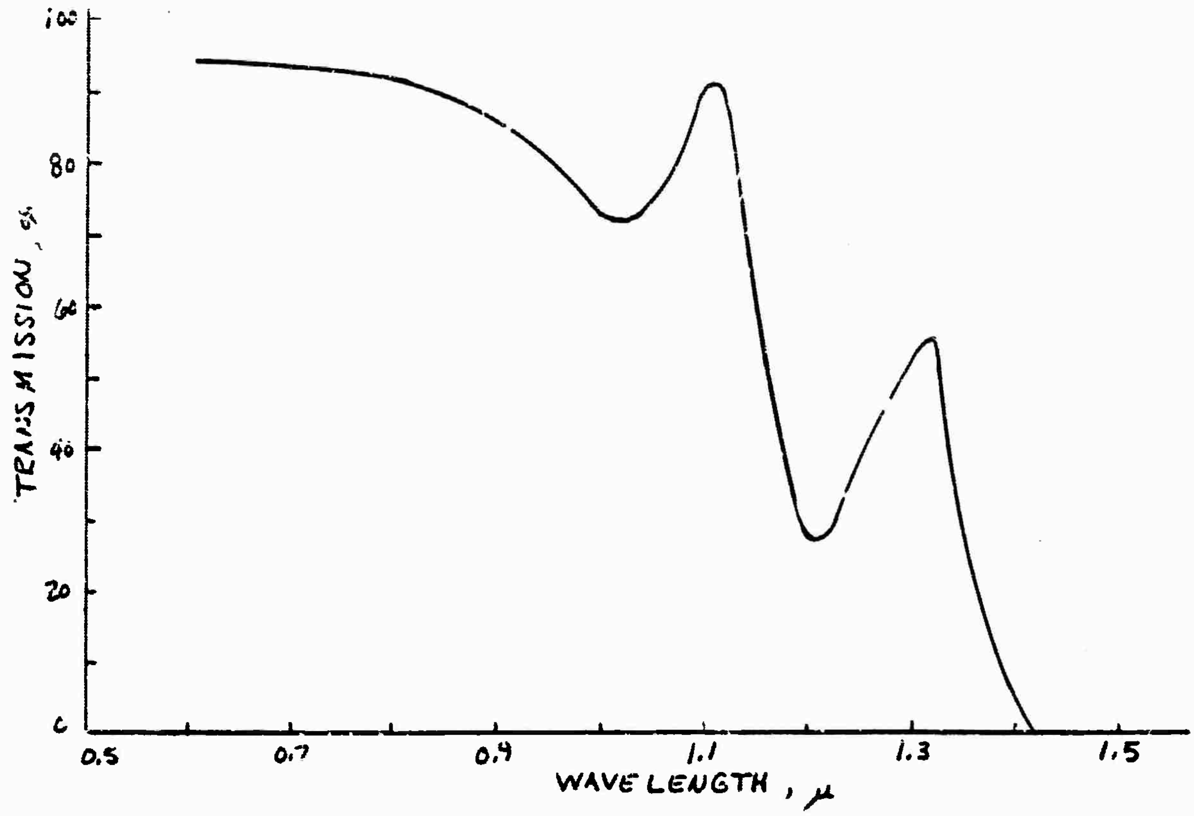

FIGURE 17 TRANSMISSION CURVE FOR 1.1 CM OF GLYCERIN

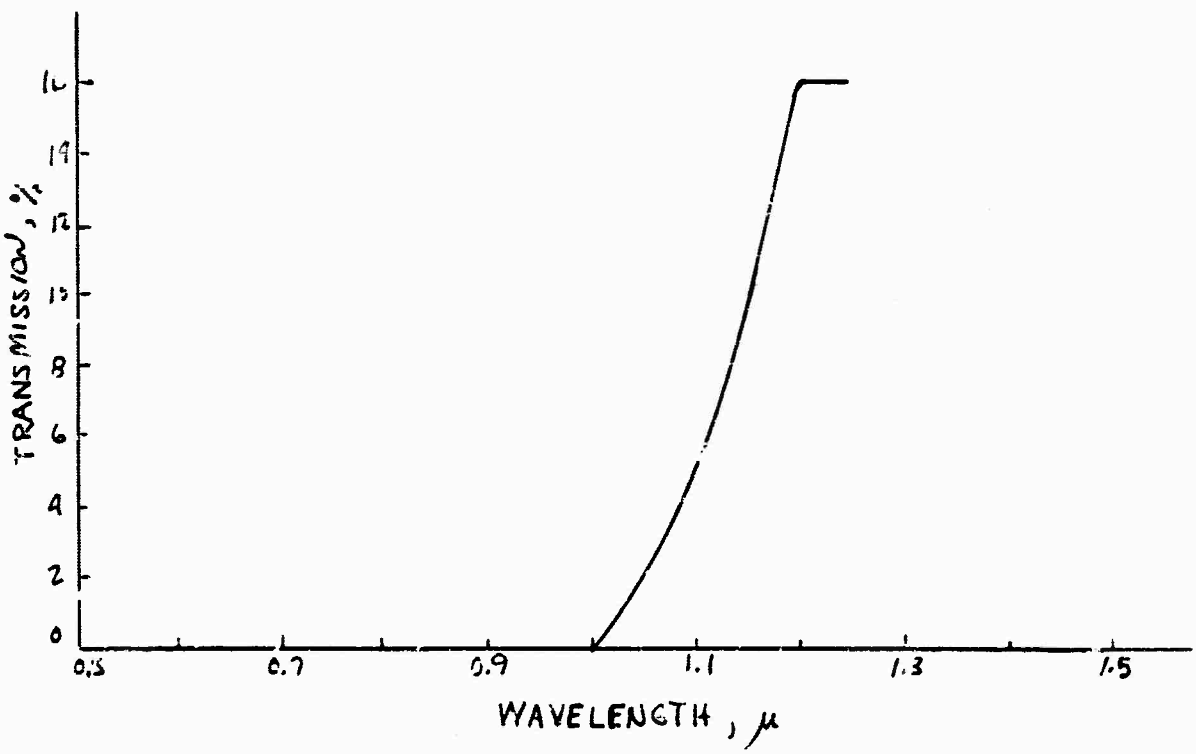

FIGURE 18 TRANSMISSION CURVE FOR 3mm OF SILICON